SEMI-ANALYTICAL CALCULATION OF ACCELERATING BEAM IN A PHOTO-INJECTOR CAVITY*

Harunori Takeda
Los Alamos National Laboratory, Los Alamos, NM 87545

Abstract

The acceleration of electrons in an injector induces a beam emittance growth. To study the emittance growth in a photo-cathode injector, we model the acceleration process analytically. Then, the analytical model is compared with numerical simulations using the PARMELA[1] code. Although the analytical model cannot represent the correct beam behavior caused by the space charge, we model the normalized emittance in an environment of a magnetic field produced from axial coils as represented by a mechanical angular momentum. We derive analytical relations from a relativistic equation of motion of a particle (envelope equation). Using the envelope equation, we study the emittance growth in the acceleration by a numerical integration.

Equation of Motion

The rf cavities accelerate particles emitted from a cathode. Representing the equation of motion with the cylindrical coordinate system (r, θ, z), we interpret particle motion as the beam envelope propagation along the positive z axis. This assumption is valid only while a cylindrically symmetric beam maintains its coherence: the particle on the envelope stays on the envelope and the particle in the beam stays in the beam along the propagation. For an axially symmetric beam propagating in an axially symmetric environment, the x emittance and the y emittance are equal and they can be represented as $\pi r_{max} v_{m\theta}$, where r_{max} and $v_{m\theta}$ are the radius and the transverse velocity, respectively, of the particle on the envelope. Later, we define the beam emittance with the coordinates of the representative particle on the envelope. This is similar to defining the emittance with the enclosing phase space ellipse. Denoting γ as the relativistic energy factor, the equation of motion that is valid from rest to relativistic velocity is given as

$$\dot{r}\dot{\gamma} - r\gamma\dot{\theta}^2 + \gamma\ddot{r} = \frac{e}{m_0 c}\left[r\dot{\theta}B_z - \dot{z}B_\theta\right] + \frac{e}{m_0}E_r(r) \quad , \qquad (1)$$

$$2\gamma\dot{r}\dot{\theta} + \dot{\gamma}r\dot{\theta} + \gamma r\ddot{\theta} = \frac{1}{r}\frac{d}{dt}\left[\gamma r^2\dot{\theta}\right] = \frac{e}{m_0 c}\left[\dot{z}B_r - \dot{r}B_z\right] \quad , \text{ and } \qquad (2)$$

$$\dot{\gamma}\dot{z} + \gamma\ddot{z} = \frac{e}{m_0}E_z + \frac{e}{m_0 c}\left[\dot{r}B_\theta - r\dot{\theta}B_r\right] \quad . \qquad (3)$$

In Eq. 1 the space charge electric field acting on a particle at beam envelope with radius r was represented as $E_r(r)\hat{r} \equiv (2q\hat{r})/(\gamma^2 rl)$, where the net charge q of particles is assumed to be uniformly distributed in a cylinder of radius r and length l ($l \gg r$). The guiding coil may have radial, azimuthal, and z components of fields given as B_r, B_θ, and B_z, respectively. In an ideal accelerator cavity operating in the TM_{010} mode, the accelerating electric field is along the z axis, and the magnetic field 90° out of phase has only an azimuthal component on a transverse plane. However, in traversing each accelerating cell, the effect of the azimuthal magnetic field cancels. If the guiding coils are aligned to the axial center of the accelerator cavity, and if we can ignore the imperfection of the cavity field, the azimuthal magnetic field can be ignored. If the effect of azimuthal magnetic field does not cancel, the emittance can grow.

Integral of Motion

The azimuthal motion (Eq. 2) can be readily integrated, and the conservation of angular momentum $m_0 K_1$ (Busch's theorem guarantees the conservation even if the B_z varies along the path) can be stated as

$$\gamma r^2\dot{\theta} + \frac{e}{2m_0 c}r^2 B_z - \frac{e}{m_0 c}\int_0^t \left[\frac{r^2}{2}\dot{B}_z + r\dot{z}B_r\right] dt = K_1 \quad . \qquad (4)$$

Normally, the canonical angular momentum is conserved if the space charge and other non-axially symmetric forces acting on the beam, which increase the emittance, can be ignored. If we measure the mechanical part of the canonical angular momentum in units of the rest momentum $m_0 c$, the mechanical angular momentum for a cylindrically symmetric beam is equal to the normalized beam emittance ϵ_n (in our argument, we consider the emittance ϵ_n defined only by the azimuthal motion of electrons).

In the integration of the mechanical angular momentum with time, we assume that the coil field is static in time and is nearly constant B_0 at position $z \geq z_0$. Defining t_0 as a time that takes to reach z_0, we divide the time integration into two domains, $t < t_0$ and $t_0 < t$. The mechanical angular momentum is expressed as

$$\gamma r^2\dot{\theta} = -\frac{e}{m_0 c}\left[\frac{r^2}{2}B_z(t) - \int_0^t \left(\frac{r^2}{2}\dot{B}_z + r\dot{z}B_r\right) dt\right] + K \quad , \qquad (5)$$

where the constant K is given with the quantities on the cathode (i subscripts):

$$K = \gamma_i r_i v_{\theta i} + \frac{e}{2m_0 c}r_i^2 B_{zi} \quad . \qquad (6)$$

With respect to the normalized emittance ϵ_n, Eq. 5 can be rewritten as

$$\epsilon_n(t) = \gamma r^2\frac{\dot{\theta}}{c} = \epsilon_n(0) - \frac{e}{m_0 c^2}\left[\frac{r^2}{2}B_z - \int_0^t \left(\frac{r^2}{2}\dot{B}_z + r\dot{z}B_r\right) dt\right] \quad , \qquad (7)$$

*Work supported and funded by the US Department of Defense, Army Strategic Defense Command, under the auspices of the US Department of Energy.

where the normalized beam emittance at cathode was given as $\epsilon_n(0) = K/c$.

Equation 7 implies that we can reduce emittance, with these conditions: (1) if the particles are emitted normal to the surface of the cathode, $\epsilon_n(0) = 0$, (2) if the particles experience no magnetic field at the cathode, $B_{zi} = 0$, and (3) if the coil field is not present at the emittance measuring position, $B_z = 0$.

If the particles are emitted normal to the cathode, and a bucking coil behind the cathode is set to cancel the magnetic field on the cathode, the emittance observed downstream $z_0 < z$ is caused by the intrinsic emittance acquired during $0 < t < t_0$ and by the emittance enhancement from the coil field B_z. The intrinsic emittance acquired up to t_0 can be expressed as

$$\epsilon_n = \frac{e}{m_0 c^2} \int_0^{t_0} \left(\frac{r^2}{2} \dot{B}_z + r\dot{z} B_r \right) dt \quad . \tag{8}$$

Using Eq. 7 and the relation $\epsilon_n(0) = \gamma r_i^2 \dot{\theta}_i / c$, the angular momentum at time t ($> t_0$) can be expressed in terms of quantities at the cathode and the intrinsic emittance as

$$\gamma r^2 \dot{\theta} + \frac{e}{2m_0 c} r^2 B_z(t) = \gamma_i r_i^2 \dot{\theta}_i + \frac{e}{2m_0 c} r_i^2 B_{zi} + c\epsilon_n \quad . \tag{9}$$

To evaluate the model (Eq. 7), we compare the numerical simulation using the PARMELA code for the injector used in the HIBAF[2] facility at Los Alamos. Table 1 and Table 2 show the injector and beam parameters for a bunch with a Gaussian temporal profile. After the 4th cell, the same 4th cell structure repeats. Figure 1 shows the PARMELA-calculated normalized emittance after the 7th cell as a function of magnetic field at the cathode. The beam kinetic energy is about 7 MeV, and the bunch charge is 0.5 nC. The slope of the emittance near the minimum, calculated from the PARMELA simulation, is in the range 0.26 to 0.33 π mm-mr/G, and the analytical coefficient $-e r_i^2/(2m_0c^2)$ equals 0.32 π mm-mr/G for a truncated Gaussian with the 0.34-cm FWHM beam. These slopes agree well.

Azimuthal Angles of Particles Emitted from a Masked Cathode

Solving Eq. 5 for $\dot{\theta}$ and integrating over time followed by a substitution of K with the emittance at cathode, we obtain an expression

$$\begin{aligned} \theta(t) = &- \frac{e}{2m_0 c} \int_0^t \frac{B(z(t))}{\gamma} dt + \left(\frac{e}{2m_0 c} \right) B_{zi} r_i^2 \int_0^t \frac{dt}{\gamma r^2} \\ &+ \left(\frac{e}{m_0 c} \right) \int_0^t \frac{dt}{\gamma(t) r^2(t)} \int_0^{t'} \left(\frac{r^2}{2} \dot{B}_z + r\dot{z} B_r \right) dt' \\ &+ c\epsilon_n(0) \int_0^t \frac{dt}{\gamma r^2} \quad . \end{aligned} \tag{10}$$

If the particles emerge normal to the photo cathode, $v_i = 0$, the beam starts with no emittance : $\epsilon_n(0) = 0$. The last term in Eq. 10 drops. For a smooth envelope, a part of radial dependence is canceled in the third term; the radial dependence also comes from the second term in Eq. 10.

If we set the magnetic field at the cathode to zero, the image at the cathode is preserved azimuthally through the varying magnetic field channel. To test the radial dependence of azimuthal angle from the second term, we set a vertical slit for a laser to produce electrons at the cathode. If the magnetic field is present at the cathode, the image at downstream could be deformed azimuthally according to the amount of change in the beam radial position. If the beam is transported with a constant radius, the azimuthal angle will show no radial dependence: the straight shape of the beam will be preserved.

Figure 2a shows the x-y profile of a beam produced with the PARMELA code at +100-G cathode field. The bunch charge is reduced for a negligible space charge effect at the narrow slit. The beam experiences a coil field change to a peak −476 G and then to a reduced −22 G at the profile point (z = 11.53 cm from the cathode). The beam is rotated counterclockwise. Because the coil field extends only up to 60 cm, the beam rotation is nearly preserved at z = 487 cm, but both ends of the profile are expanded counterclockwise. This is shown in Fig. 2b. If we apply an opposite magnetic field, we observe a clockwise beam rotation. The wings also extend clockwise. With no magnetic field on the cathode, the straight shape is preserved.

TABLE 1
Injector Parameters

Cell	Average E Field (MV/m)	Length (cm)
1	22.07	6.02
2	11.14	11.53
3	8.0	11.53
4	5.46	11.53

TABLE 2
Beam Parameters

Bunch Charge (nC)	Bunch Length (ps)	Spot Radius on Cathode (cm)
0.5	35 ($2\sigma_z$=12 ps)	0.42

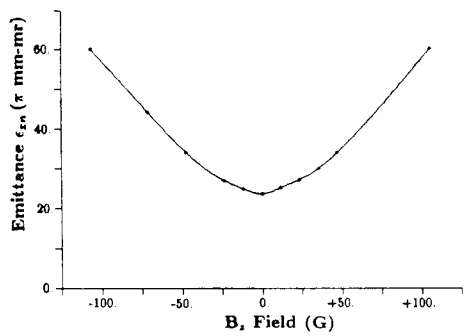

Fig. 1. The normalized emittance minimizes at zero cathode magnetic field.

Numerical Integration of Motion

In an actual photo-injector, the electric field acting on the particle varies according to each cavity gap voltage. Also the

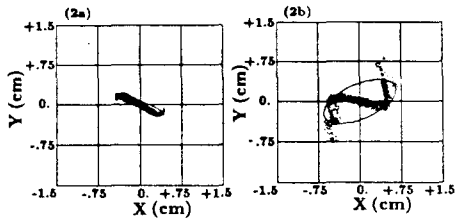

Fig. 2. The beam rotation by the coil field: observed at Z = 11.53 cm (2a), at Z = 487 cm (2b).

particles near the photo-cathode experience a large phase slip with respect to the rf wave. In our envelope model, we include the gap voltage at each cavity, but the transit time effect is averaged. Assuming that the reference particle is always on the beam envelope, we integrate the envelope equations Eqs. 1-3, without B_θ term.

For the HIBAF injector, as an example, Fig. 3 shows the profile of magnetic field $B(z)$ from field coil along the injector. The step-like accelerating electric field E_z, Fig. 4, is also shown similarly. We compare the results from test particle integration with the PARMELA simulation.

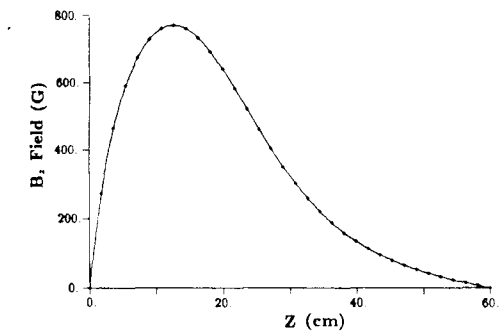

Fig. 3. The coil field, B_z, along the z axis.

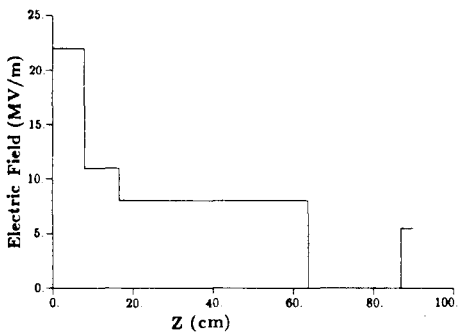

Fig. 4. The accelerating E field along the z axis.

We assume the coil field peaked at the same 769.1 G for the test particle calculation as was assumed in the PARMELA calculation. The radial profile for the test particle is shown in Fig. 5a. The corresponding PARMELA-calculated envelope (Fig. 5b) does not have a rapid initial expansion of envelope as shown in Fig. 5a. The normalized emittance from the test particle integration (Fig. 6a) has a profile similar to the PARMELA result, which calculated four times the RMS emittance (Fig. 6b). However, because of the conservation of canonical angular momentum, the assumed axial symmetry in the model produced zero emittance where the coil field is terminated. The magnitude is about two times larger than the emittance calculated with the PARMELA code. This is because the simplified space charge model does not represent well the profile of the bunch, which was Gaussian both in temporal and cross-sectional dimensions.

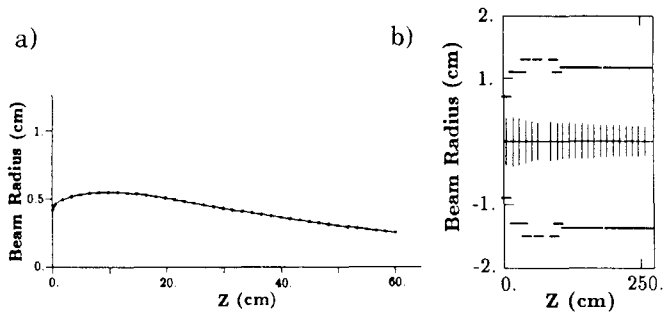

Fig. 5. The beam envelopes from the envelope model (5a) and from the PARMELA code (5b).

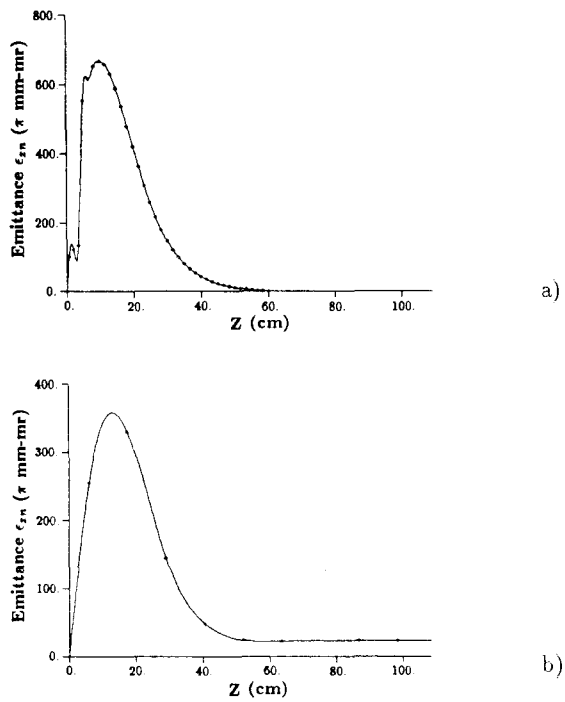

Fig. 6. Normalized emittances from the envelope model (6a) and from the PARMELA code (6b).

References

1. "Computer Codes for Particle Accelerator Design and Analysis: A Compendium," Los Alamos National Laboratory report LA-UR-90-1766 (May 1990), p.137.
2. W. D. Cornelius et al., "The Los Alamos High-Brightness Accelerator FEL Facility," 11th International Free Electron Laser Conference, Naples, Florida, August 28-September 1, 1989.